A New Method for Multifractal Spectrum Estimation with Applications to Texture Description

Jacques Lévy Véhel Michel Tesmer
Regularity Team, INRIA Saclay and MAS Laboratory,
Ecole Centrale Paris, Grande Voie des Vignes,
92295 Chatenay-Malabry Cedex, France

Abstract

Multifractal analysis is a tool allowing for a detailed analysis of the singularity structure of an image, both at the local and global levels. It has been used in image processing for various purposes including classification, denoising, and edge detection. One of the most important steps is the computation of multifractal spectrum. While non-parametric estimation methods exist, techniques assuming that the image displays some sort of multifractal scaling generally give better results, since they take advantage of the structure present in the data. In this work a robust estimation procedure is presented for computing the large deviation (LD) multifractal spectrum, as well as an extension called the Undecimated Large Deviation (ULD) spectrum. Both methods are put to use on artificial and real images. The results show that multifractal spectra estimated with our method are strikingly different in the case of textured natural images and face images. In addition, multifractal spectra seem to be able to classify natural textures.

1. Introduction

Multifractal analysis is concerned with describing the regularity of functions, both from a local and global point of view. More precisely, performing the multifractal analysis of an image I amounts to computing a so-called *multifractal spectrum*: This is a function $f(\alpha)$ which gives, for every value of α, the "amount" of points in the support of the image where I has "singularity" α. Singular here means that the image is not smooth, that is, C^∞, at the considered point and α roughly gives the degree of (fractional) differentiability. See section 2 for precise definitions. Multifractal analysis is a topic that attracts a lot of interest in mathematics, physics [2, 12], financial analysis [13], the study of Internet traffic [10], astronomy, and a number of other fields. Indeed, it is powerful tool that allows one to analyse finely the structure of irregular objects such as turbulence, financial records, TCP logs or galaxies distribution.

Multifractal analysis can be applied to any object, independent of the assumption of fractality. However, it will yield interesting results only for data displaying a strongly irregular behaviour. This is in particular the case for many natural images.

Multifractal analysis has been applied in image processing for edge detection, denoising and change detection [4–9]. The basic idea is that many structures present in an image have a particular signature in the multifractal spectrum. Edges, for instance, correspond to a specific subset of singularity values, characterized by the fact that the geometry of the corresponding points is that of a set of lines. Denoising may be performed by translating the multifractal spectrum to the larger values of α.

A critical step in the multifractal analysis of an image is of course that of estimating the multifractal spectrum. Several estimation procedures have been proposed (see e.g. [1, 3, 14]). While some do not make any assumption on the structure of the data, most of them hypothesize some sort of *multifractal scaling*: This roughly means that properly defined subsets of the support of the image display a fractal behaviour (see section 2.2 for a precise statement). Assumption-free approaches will be preferred when large samples are available and when one does not want to restrict the domain of application of multifractal analysis. The second kind of methods yield more robust estimation results, provided the assumption of multifractal scaling has been verified.

The main purpose of this paper is to investigate which kind of images do possess multifractal scaling and to propose a robust estimation scheme for images exhibiting such scaling. Checking whether an image displays multifractal scaling is important in applications, as it conditions the method used for estimating the multifractal spectrum: If one is confident that the set of images to be processed exhibit multifractal scaling, then the more efficient parametric estimation procedures may be used to obtain more precise results. It seems intuitive that strongly textured images as well as outdoor scenes are more likely to display multifractal scaling than indoor images or pictures of, *e.g.*, faces, a fact that we verify experimentally below.

The remaining of this work is organized as follows: Section 2 recalls the basics of multifractal analysis, focusing on the so-called *large deviation spectrum*, which is the most useful spectrum in applications to image processing. Section 3 details our algorithm for *coarse-grained multifractal spectrum* estimation. The computation of an extension called Undecimated Large Deviation Spectrum is also described. An experiment on a typical multifractal image, called a binomial measure, is briefly studied in section 4. Section 5 presents the results of assessment of multifractal scaling as well as of spectra computations on a large number images: Pure textures, natural landscapes and faces. Section 6 presents the conclusions of our work.

2. Multifractal Analysis

Multifractal analysis gives a description of the singularities of an image from a local and global point of view simultaneously. In that perspective, various *multifractal spectra* are defined, each one putting emphasis on a particular aspect of the singularity structure. We restrict in this work to the large deviation multifractal spectrum, whose definition we recall now.

2.1. The Large Deviation Multifractal Spectrum

Assuming without loss of generality that the support of the image I is $[0,1]^2$, consider the sequence of partitions of $[0,1]^2$ by dyadic squares $J_n^{k,l} = [k2^{-n}, (k+1)2^{-n}] \times [l2^{-n}, (l+1)2^{-n}]$. To each $J_n^{k,l}$, one associates a positive real number $Y_n^{k,l}$ that gives an indication of the "activity" of I inside $J_n^{k,l}$. Classical choices for $Y_n^{k,l}$ include the sum of the gray levels inside $J_n^{k,l}$, the oscillation of I inside $J_n^{k,l}$, or the modulus of the wavelet coefficients of I at scale n and location (k,l).

The *coarse-grained* Hölder exponents of I are, by definition, the numbers

$$\alpha_n^{k,l} = \frac{-\log Y_n^{k,l}}{n \log 2}. \tag{1}$$

For any real number α and any positive number ε, let $N_\alpha(\varepsilon, n)$ denote the number of 2^{-n} dyadic squares such that $|\alpha_n^{k,l} - \alpha| \leq \varepsilon$. The *large deviation spectrum* of I is defined as

$$f(\alpha) = \lim_{\varepsilon \to 0} \left(\limsup_{n \to \infty} \frac{\log N_\alpha(\varepsilon, n)}{n \log 2} \right), \tag{2}$$

with the convention that $\log N_\alpha(\varepsilon, n)/n \log 2 = -\infty$ if $N_\alpha(\varepsilon, n) = 0$. The "pre-asymptotic" functions

$$f_\varepsilon^n(\alpha) = \frac{\log N_\alpha(\varepsilon, n)}{n \log 2}$$

are called the *coarse-grained spectra* of I. From the definition, it is easy to see that f takes values in $-\infty \cup [0,2]$.

The heuristic meaning of f is the following: For a fixed resolution n, pick at random a dyadic square in $[0,1]^2$. Then, for n large enough, the probability that the chosen square has a coarse-grained exponent roughly equal to α is of the order of $2^{-n(2-f(\alpha))}$. In particular, if $f(\alpha) < 2$, then this probability vanishes exponentially fast as n tends to infinity, hence the name "large deviation spectrum". If, for instance, $f(\alpha) = 1$, this probability decays at the same rate as the one of hitting a point on a contour at resolution n. See [8] for more on the definition and properties of the large deviation multifractal spectrum.

2.2. Multifractal Scaling

The "true" spectrum is obtained as the upper limit of the coarse-grained spectra f_ε^n when the resolution tends to infinity. As a consequence, it cannot be computed on real-world data. One way to estimate it at finite resolutions is to use a algorithm called "liminf regression", that will not be considered in this work [11]. The advantage of using a liminf regression is that it does not require any assumption on the structure of the image. The price to pay is that the estimation may require a

large number of points, i.e., the convergence may be quite slow. This work is focused on another approach, where some assumptions are made about the data. We will say that an image sampled at resolution n exhibits *multifractal scaling* if the coarse-grained spectra at resolutions $n, n-1, \ldots, n-p$ are similar for some $p > 1$:

$$f^{\varepsilon}_{n-i} \simeq f^{\varepsilon}_{n-j},\ i, j = 0 \ldots p,$$

where the symbol $a \simeq b$ means that some norm of the difference $a - b$ is "small". This assumption amounts to stating that, at the p finest available resolutions, the image behaves as if a "steady state" has been reached in terms of multifractal analysis. In other words, the statistics of the coarse-grained Hölder exponents all exhibit a scaling law with respect to resolution. The estimation of the spectrum is then of course considerably simplified, since it seems reasonable to view the common value of these spectra as the multifractal spectrum of the image. The following section details an algorithm implementing these ideas.

3. Estimating the Large Deviation Multifractal Spectrum

3.1 Outline of the method

To verify that an image possesses multifractal scaling, one needs to estimate in a reliable way the coarse-grained spectra f^{ε}_{n-i} for increasing values of i.

Computing these estimations requires to choose carefully the value of ε. Indeed, while the mathematical definition lets ε go to 0, in practice, one must fix a specific positive value when dealing with finite resolution data. Setting $\varepsilon = 0$ when n is finite would indeed result in a spectrum that would be equal to $-\infty$ except at a finite number of points. The value of ε serves roughly the same purpose as the kernel width in classical density estimation, except that here we consider a bi-logarithmic sequence of renormalizations of densities.

The main idea of this work is to choose ε so as to obtain the best possible estimation. Note that there is no reason why the value of ε should be kept constant across scales. Indeed, in density estimation, the width of the kernel is a decreasing function of n. In order to find an optimal vector $\varepsilon = (\varepsilon_1, \ldots, \varepsilon_n)$ of values of ε that will lead to a robust estimation, we investigated the following criteria:

- Correlation of α_{mod}: During the computation procedure the spectra at all scales are aligned so that the locations of their maximum all fall at the same point called α_{mod}. This point is supposed to approximate the Hölder exponent associated to the maximum of the "true" spectrum. It is computed by regressing the locations of the spectra maxima ($\tilde{\alpha}_{\eta_i}$) with respect to scale. In order to obtain an accurate value of α_{mod}, the values $\tilde{\alpha}_{\eta_i}$ should be strongly correlated across scales. Therefore, this criterion chooses ε so as to maximize the correlation among the $\tilde{\alpha}_{\eta_i}$. The rationale for this criterion is that the estimation at the maximum is the most robust, and thus should be used for aligning all the spectra.
- Distance: As mentioned in section 2.2, an image will be said to display a multifractal behaviour if the coarse-grained spectra at different resolutions are similar. This criterion aims at minimizing the distances among the spectra at all scales. This quantity is defined as the sum of the L^2 distances $\sum_i \sum_j (f^{\varepsilon_{n-i}}_{n-i} - f^{\varepsilon_{n-j}}_{n-j})^2$.
- Correlation of α_{mod} & Distance: This criterion is a linear combination of both the ones above, with a parameter $\beta \in [0, 1]$ that controls the relevance of each term in the optimization criterion. The criterion has the following expression:

$$f_{obj} = \beta \operatorname{corr}(\log \mu_{\tilde{\alpha}_\eta}, \log \eta) + (1 - \beta) \sum_i \sum_j (f^{\varepsilon_{n-i}}_{n-i} - f^{\varepsilon_{n-j}}_{n-j})^2. \tag{3}$$

Thus our estimation procedure goes as follows: Fix $\varepsilon = (\varepsilon_1, \ldots, \varepsilon_n)$, then compute all the coarse-grained spectra $f^{\varepsilon_{n-i}}_{n-i}$. Compute the sum of the L^2 distances $\sum_i \sum_j (f^{\varepsilon_{n-i}}_{n-i} - f^{\varepsilon_{n-j}}_{n-j})^2$ among all spectra, as well as, for each scale, $\tilde{\alpha}_\eta = \operatorname{argmax}_{\eta,\alpha} N_\alpha(\varepsilon, \eta)$, and the correlation between $\log \mu_{\tilde{\alpha}_\eta}$ and $\log \eta$. Finally, applying one of the three optimization criteria above, obtain the optimal $\varepsilon^* = (\varepsilon^*_1, \ldots, \varepsilon^*_n)$ through a standard gradient descent method.

Once the large deviation multifractal spectrum have been computed in an optimal way at several resolutions, a comparison of the graphs allows to detect multifractal scaling.

3.2 Spectrum Estimation Algorithm

The large deviation spectrum is defined by the following power law:

$$N_\eta(\alpha_i) = K_\eta \, 2^{\log \overline{N_\eta} \, f(\alpha_i)} \tag{4}$$

where $N_\eta(\alpha_i)$ is the number of squares of size η whose coarse-grained exponent is between $\alpha_i - \varepsilon$ and $\alpha_i + \varepsilon$, K_η is a normalizing constant, and $\overline{N_\eta}$ is the total number of squares of size η *i.e.*

$$\sum_i N_\eta(\alpha_i) = \overline{N_\eta}. \tag{5}$$

Taking logarithms, (4) reads:

$$\frac{\log N_\eta(\alpha_i)}{\log \overline{N_\eta}} = \frac{\log K_\eta}{\log \overline{N_\eta}} + f(\alpha_i) \tag{6}$$

In most works the constant term K_η is considered negligible and it is removed from (4). In this case estimation reduces to computing the slope of the mean-square regression of $\log N_\eta(\alpha_i)$ *versus* $\log \overline{N_\eta}$.

Here, we will considered the whole expression in (6). Combining (5) and (6), we obtain a nonlinear equations system for computing the LD spectrum:

$$f(\alpha_i) - \frac{\log \sum 2^{\log \overline{N_\eta} \, f(\alpha_i)}}{\log \overline{N_\eta}} - \frac{\log N_\eta(\alpha_i)}{\log \overline{N_\eta}} + 1 = 0 \tag{7}$$

The different steps of the proposed method applied to a generic image of size $[N \times M]$ are as follows:

1. **Image normalization**
   The gray level values are normalized into the interval $[0, 1]$.
2. **Coarse-grained Hölder exponents computation**
   The image is divided in boxes of size η_i (scales). In each box, the coarse-grained exponents are computed using (1). The coefficients for scale i are arranged into a vector of size $\frac{N \cdot M}{\eta_i^2}$. The final output of this step is thus a coarse-grained Hölder exponents triangular array.
3. **Histogram building**
   In order to compute a first pass of histograms $N_\alpha(\varepsilon, \eta_i)$, an initial value for ε_0^i is chosen at each scale: it is set to half the maximum distance between two adjacent coarse-grained exponents. The histograms $N_\alpha(\varepsilon_0, \eta_i)$ are then computed for all scales.
4. α_{mod} **computation**
   The values $\tilde{\alpha}_{\eta_i}$ where the maxima of the histograms at each scale is reached are computed. A linear regression of these values with respect to scale is then performed. This yields a value α_{mod}. This number is used to re-align the spectra at all scales, so that they all reach their maximum at α_{mod}. In that view, all coarse-grained exponent values are simply shifted by $\alpha_{mod} - \tilde{\alpha}_{\eta_i}$ at scale i.
5. ε **optimization**
   A standard gradient optimization procedure is used to estimate the vector $\varepsilon^* = (\varepsilon_1^*, \ldots, \varepsilon_n^*)$ that satisfies one of the criteria explained in section 3.1.
6. **Histogram re-computation**
   Steps 3 and 4 are performed again using the optimal ε^*.
7. **Final spectrum**
   The system (7) is solved to obtain the LD multifractal spectrum.

Let us now explain briefly the idea of the Undecimated Large Deviation spectrum: instead of partitioning at scale i the image in boxes of size η_i, one uses a moving box of the same size: Thus, at each location in the image, one centres a box of size η_i to compute the coarse-grained exponents. As a result, the set of exponents at each scale and each location is matrix with same size as the original image, rather than a triangular array as it was in the original procedure.

Our method has been implemented in the *Fraclab* toolbox [11]. This is a free Matlab toolbox, that provides an extensive set of fractal and multifractal methods to performs image and signal processing tasks. FracLab thus permits to reproduce the results presented in this work, as well as to compute various other (multi-)fractal parameters that are used *e.g.* for classification, segmentation, denoising or interpolation.

4. Testing Experiments

We show in this section an experiment on a simple multifractal image called a binomial measure [1]. Such an image allows us to assess the performance of our estimation scheme. Figure 1 displays the 2D binomial image along with its theoretical spectrum.

Figure 2 shows the histograms computed with the initial value of ε (maximum distance between two adjacent Hölder exponents) on the left and the result of the next step, corresponding to the computation of α_{mod} value and the shift of the histograms on the right.

Figure 3 shows the histogram after ε optimization which has the effect of smoothing the histograms. On Figure 4 are displayed the spectra computed using the simplified version the value of K along with the one using (7).

Figure 5 shows the result when computing the ULD spectrum. It appears that the LD spectrum yields a smoother spectra, while the smaller values are more precisely estimated in the ULD method.

Finally, Figure 6 shows the comparison of the theoretical spectrum with the proposed methods, LD and ULD. It can be seen that both estimations are similar to the theoretical one. Although the ULD method exhibits a noisier estimation and a small shift to the left as compared to LD, its amplitude is closer to the theoretical spectrum.

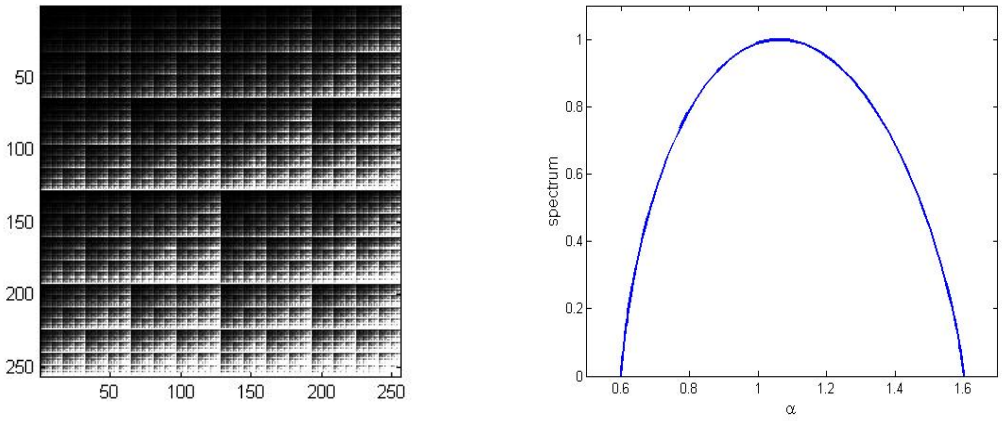

Fig. 1. Binomial measure image and its theoretical spectrum.

5. Numerical Experiments

As a first application of our method, we seek to check which kind of images display multifractal scaling, in the sense of having similar spectra over a range of scales. It seems intuitively clear that images that are mostly smooth, like images of faces, will not exhibit this property, while images of natural textures or landscapes should.

To verify these thoughts, we estimated the LD and ULD spectra on several images: 60 texture images, 60 outdoor scenes, and 12 images of faces[1]. Only 12 face images were considered because the results were clearly negative in all cases: Typical results on two face images, displayed on Figure 7, are shown on Figure 8. As it can be seen, the coarse-grained spectra are quite different at each scale, implying that the multifractal assumption does not hold here.

Figures 9 and 11 show 6 typical texture images used in the experiments. Their LD and ULD spectra are displayed on Figures 10 and 14. Both spectra exhibit for all images a strong similarity across scales. The same conclusion hold for the outdoor images (Figures 12 and 13), whose spectra are shown on Figures 15 and 16. One may thus consider such highly irregular images as truly multifractal.

As a further experiment, we tested whether the multifractality property depends on the choice of the $Y_n^{k,l}$, *i.e.* the way the "activity" inside a box is measured. We used three different measures: the first one consists in setting $Y_n^{k,l}$ equal to the sum

[1] We only display the results for 6 textures, 6 outdoor scenes and 2 faces for lack of space. Results on the other images were very similar.

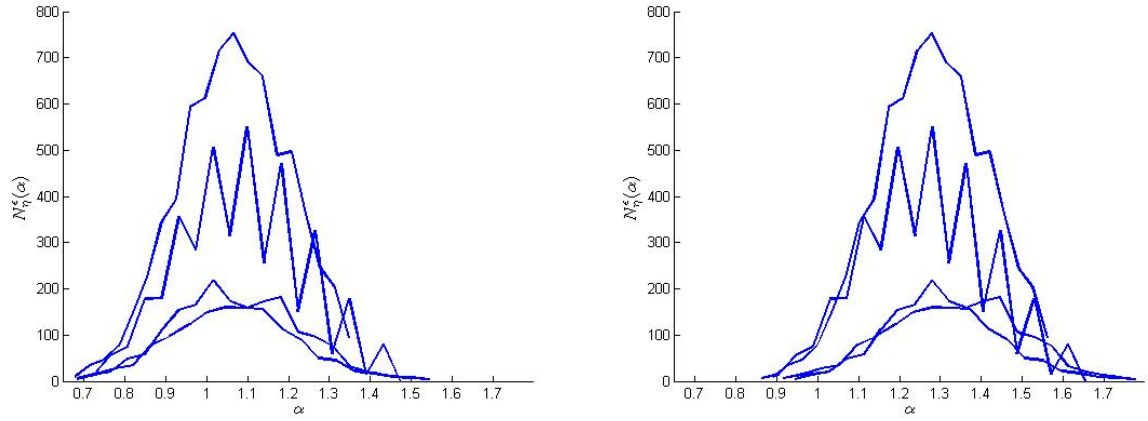

Fig. 2. Spectrum building process for the binomial measure image (steps 3, 4). Left figure: Histogram using initial epsilon. Right figure: Histogram centred around initial α_{mod}.

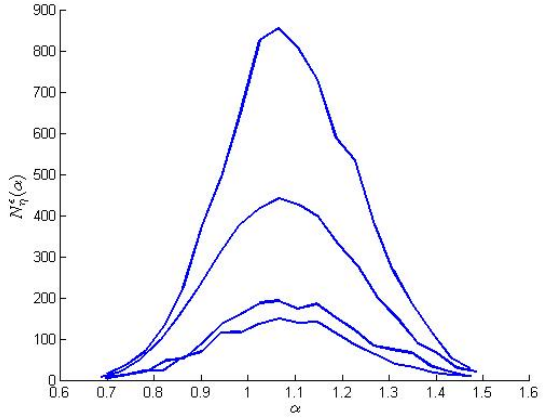

Fig. 3. Spectrum building process for the binomial measure image (steps 5, 6). Histogram with optimized epsilon.

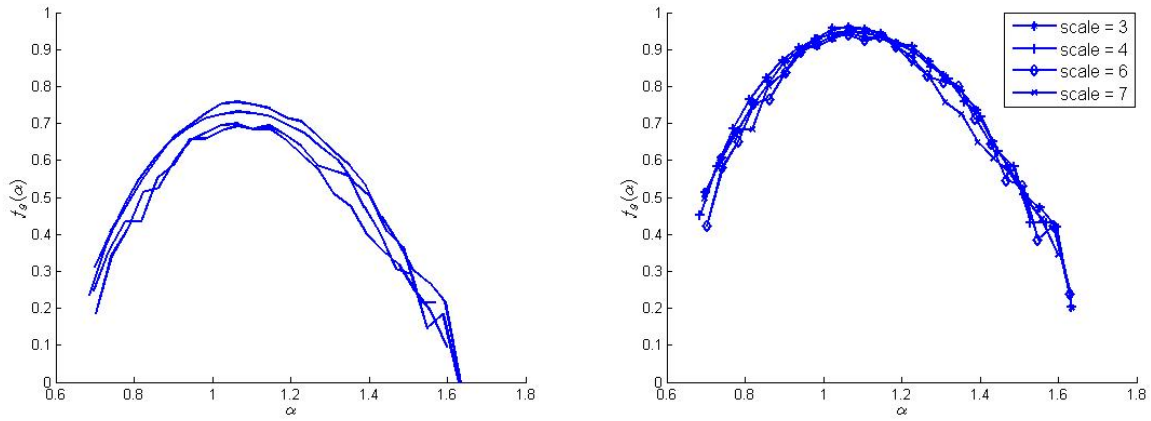

Fig. 4. Spectrum estimation for the binomial measure image (step 7). Left: Spectrum rescaled without constant K_n. Right: Spectrum rescaled with K_n.

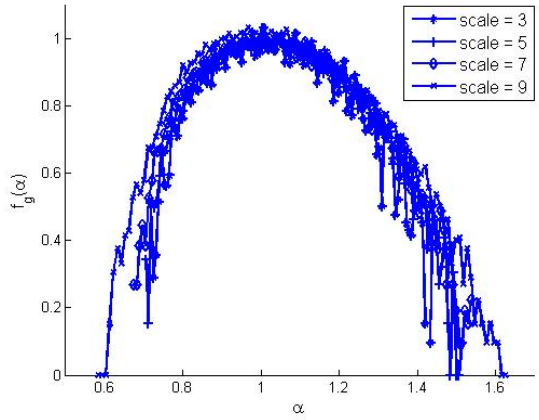

Fig. 5. Spectrum estimation for the binomial measure image, by using the Undecimated large deviation method.

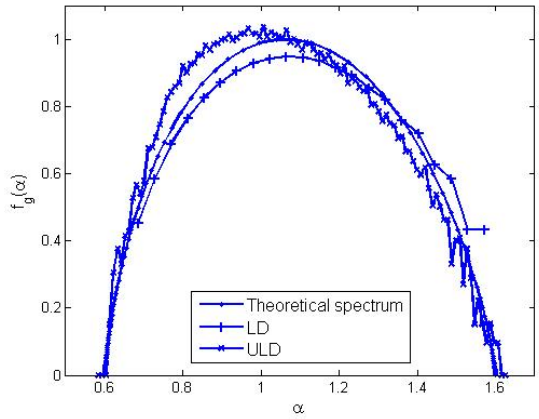

Fig. 6. Comparison of binomial measure theoretical spectrum with the estimations of the proposed methods, LD and ULD.

of the grey level inside a box (referred to as "Sum" in the captions). For the second one, we use the oscillation inside the box, *i.e.* the difference between the largest and smallest grey level (referred to as "Osc" in the captions). Finally, the third one takes $Y_n^{k,l}$ to be the mean of the grey levels in the box (referred to as "Mean" in the captions). As is apparent from the figures, the multifractal quality of the images is not dependent on the way to measure the activity. This suggests that multifractality is a robust property of textured images.

We note finally that the spectra for different images are quite distinct in shape and in location/amplitude. This indicates that they may serve as a basis for classification. This will the topic of a subsequent study.

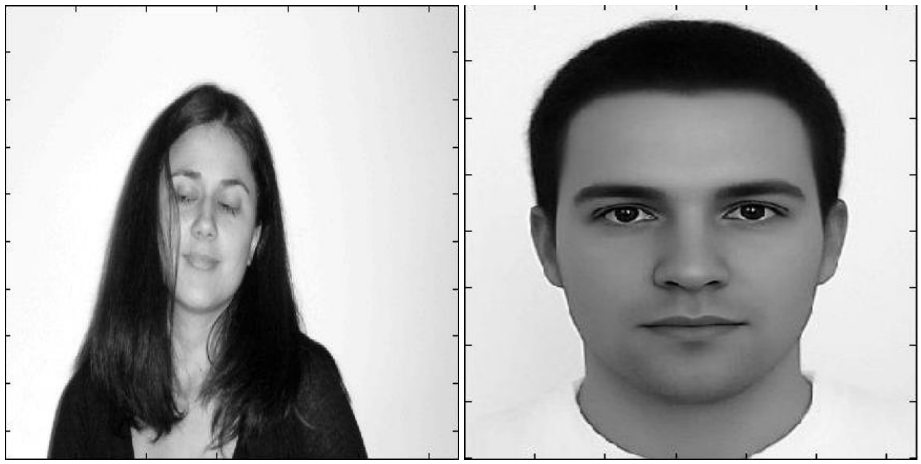

Fig. 7. Typical face images used for the estimation of the coarse-grained spectra.

6. Conclusions

Checking whether a given image displays multifractal scaling or not is useful in several applications: Multifractal images may be processed with various techniques for purposes of classification, segmentation, interpolation or denoising. The first

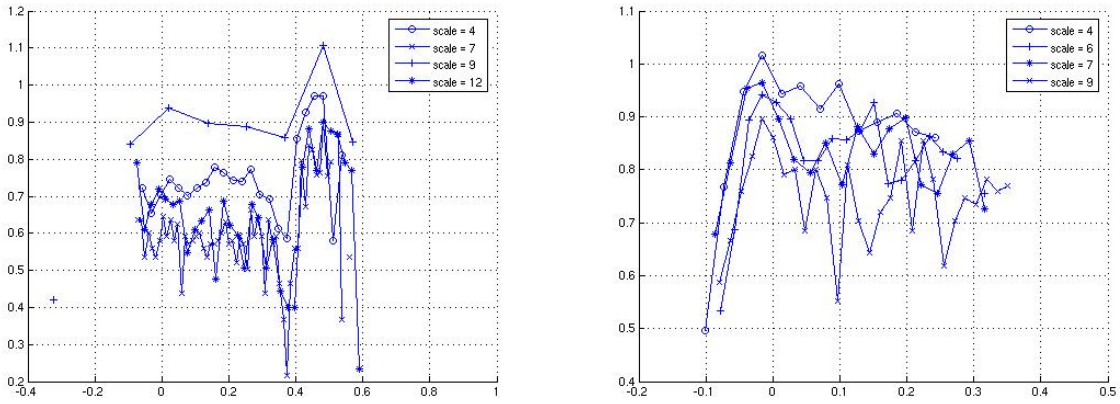

Fig. 8. Typical coarse-grained spectra for face images.

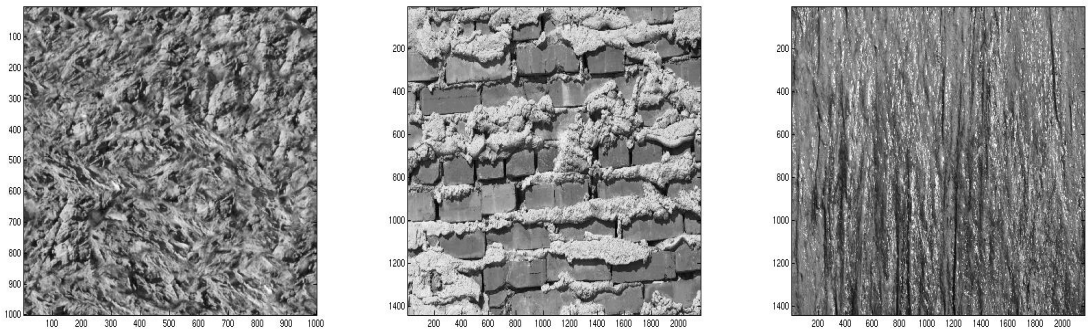

Fig. 9. Typical texture images used for the estimation of the coarse-grained spectra. Sum measure (Sum).

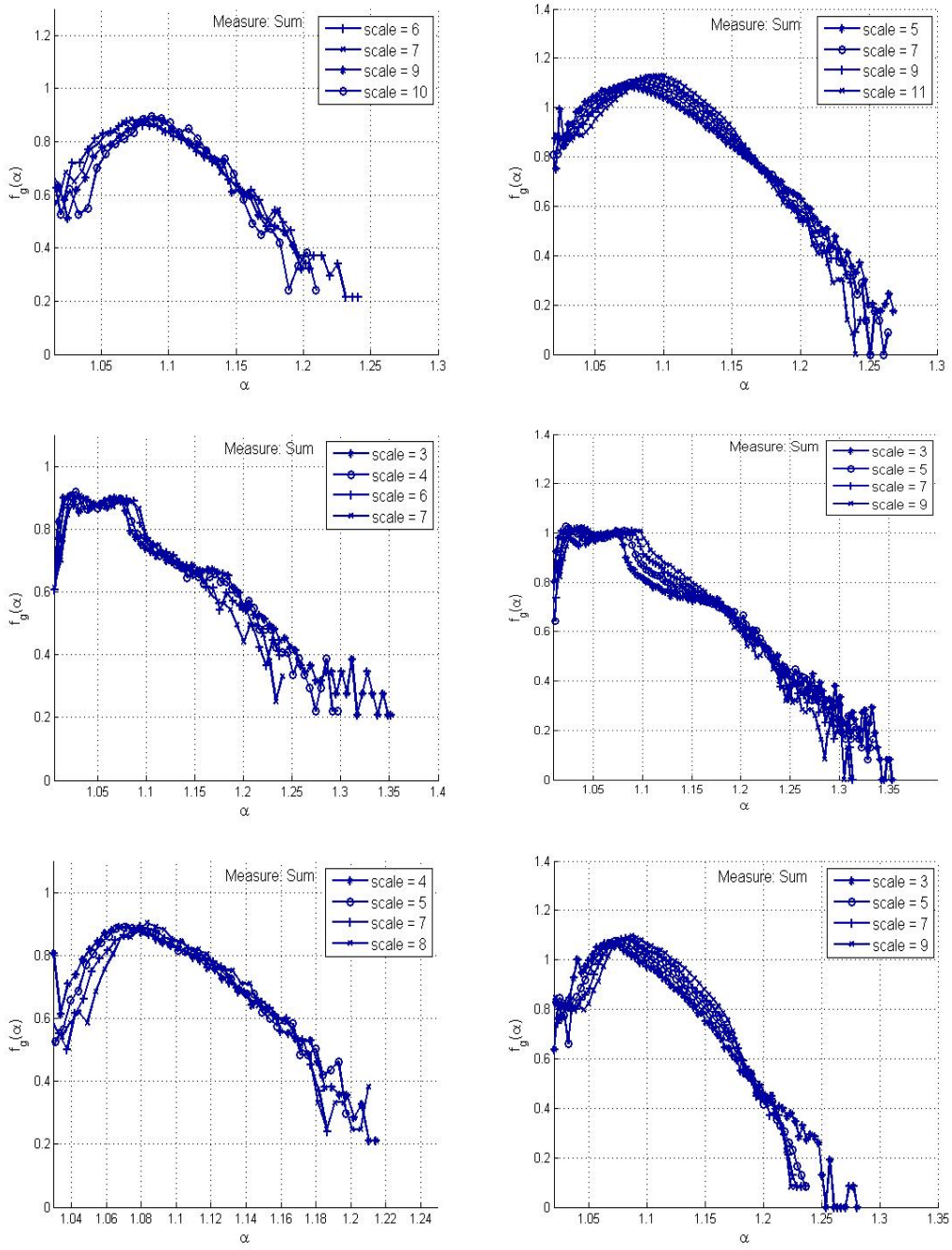

Fig. 10. Coarse-grained spectra for the texture images of Figure 9. Left column graphs: LD spectra, right column graphs: ULD spectra.

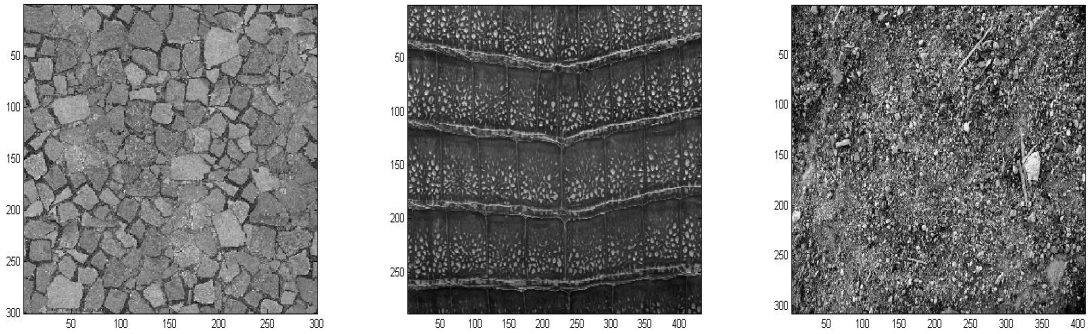

Fig. 11. Typical texture images used for the estimation of the coarse-grained spectra. Oscillation measure (Osc).

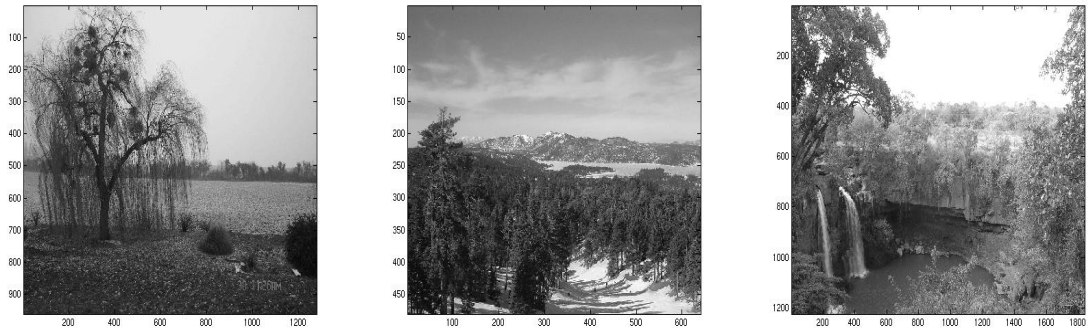

Fig. 12. Typical outdoor images used for the estimation of the coarse-grained spectra. Sum measure (Sum).

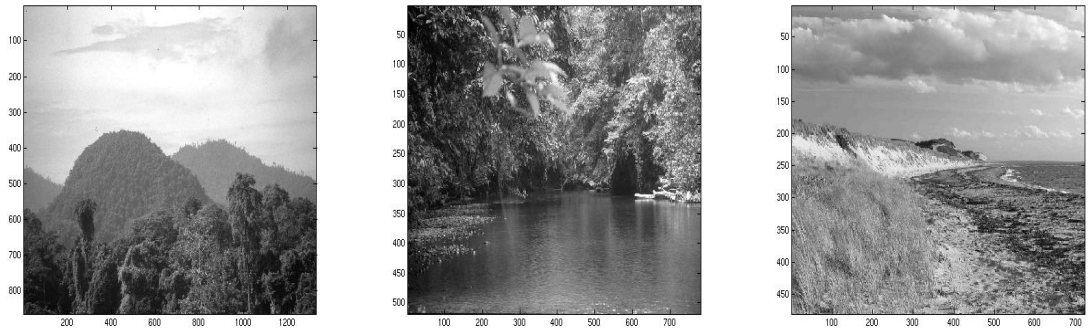

Fig. 13. Typical outdoor images used for the estimation of the coarse-grained spectra. Mean measure (Mean).

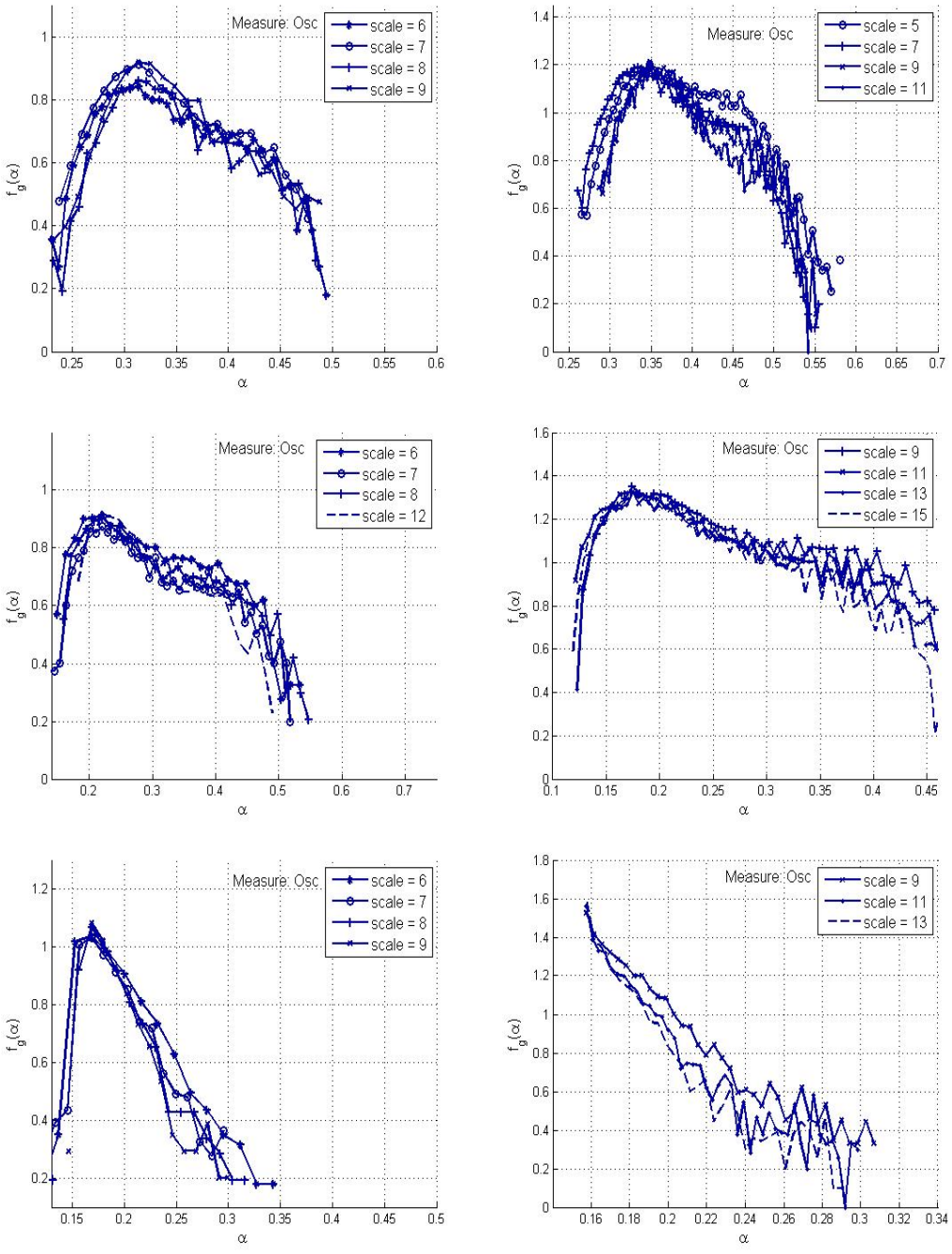

Fig. 14. Coarse-grained spectra for the texture images of Figure 11. Left column graphs: LD spectra, right column graphs: ULD spectra.

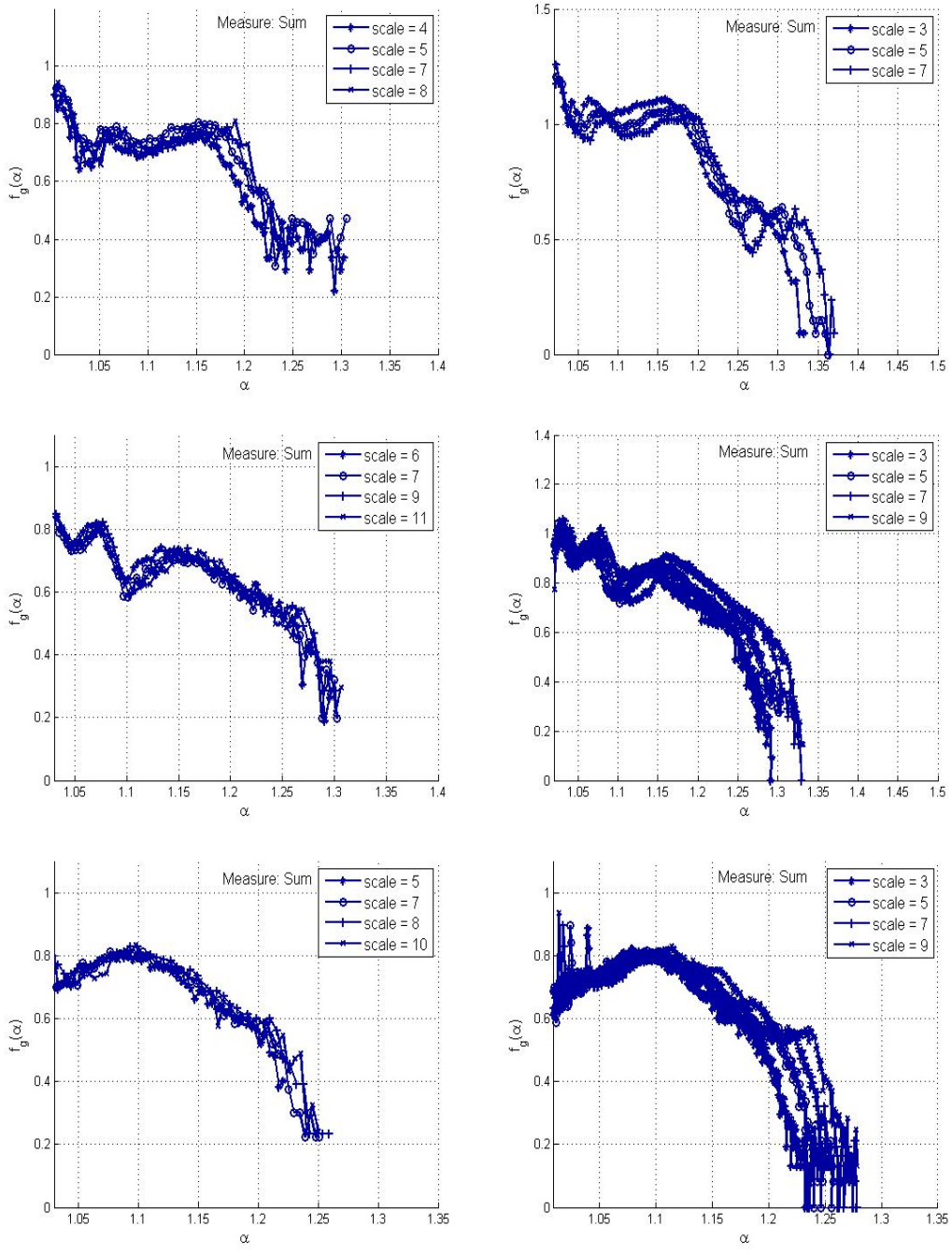

Fig. 15. Coarse-grained spectra for the outdoor images of Figure 12. Left column graphs: LD spectra, right column graphs: ULD spectra.

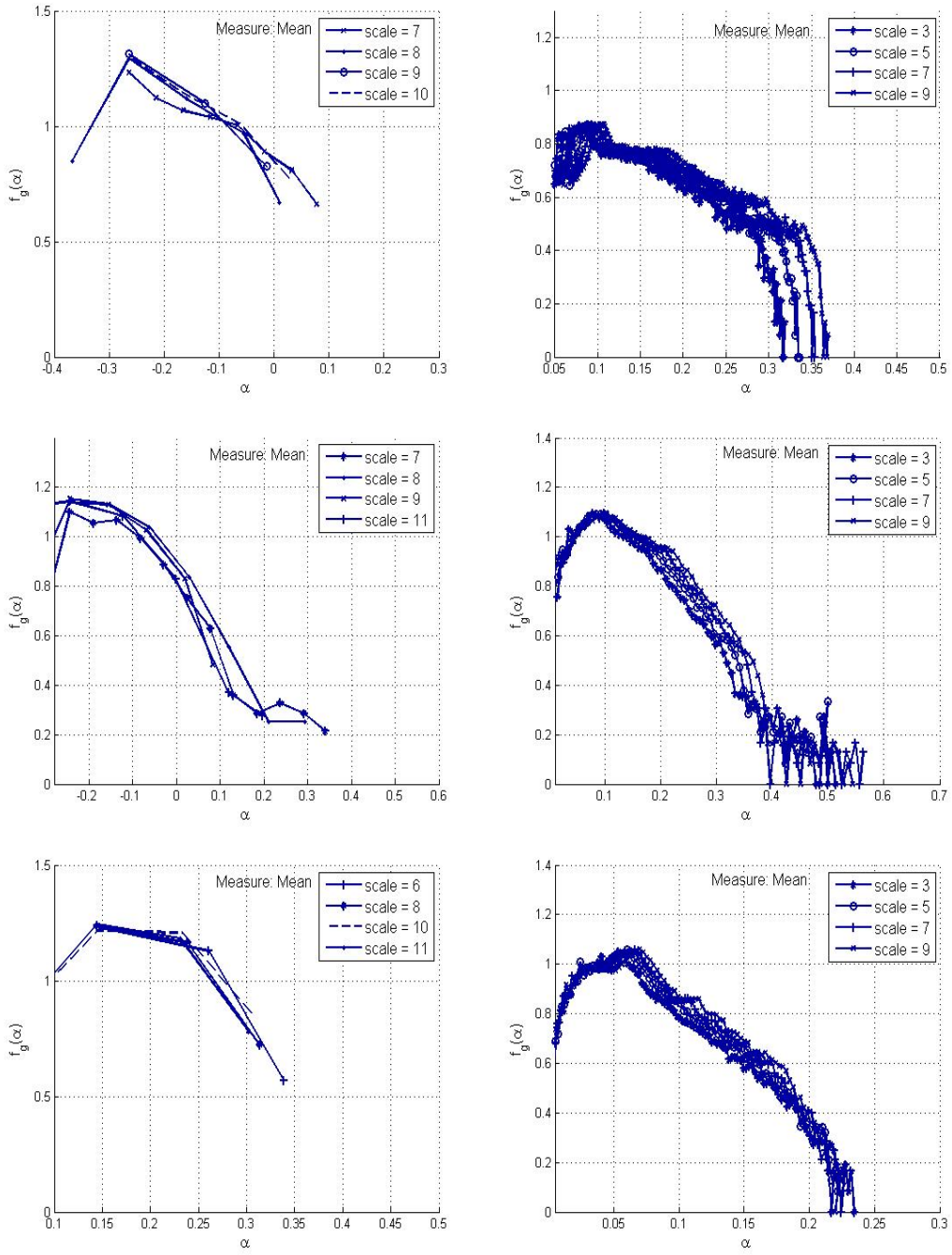

Fig. 16. Coarse-grained spectra for the outdoor images of Figure 13. Left column graphs: LD spectra, right column graphs: ULD spectra.

step to assess such a property is to be able to estimate in a robust way the multifractal spectrum. We have proposed a method that fulfils this goal by a careful analysis of the definition of the large definition multifractal spectrum.

As an application, we have shown that, not surprisingly, images of faces do not exhibit multifractal scaling, while pure textures and outdoor scenes do. Such a property is robust across scales and with respect to how one measure the activity of the image. In addition, both the LD and ULD spectra give similar results.

The next step will be to use our estimator for purposes of classification and segmentation.

References

1. C. J. G. Evertsz, B. Mandelbrot, "Multifractal Measures", in *Chaos and Fractals: New Frontiers in Science*, Springer-Verlag, pp. 921-953, 1992.
2. U. Frisch, G. Parisi, "Fully Developed Turbulence and Intermittency", in Proc. *International Summer School Phys., Enrico Fermi*, North Holland, pp. 84-88, 1985.
3. J. Lévy Véhel, "Numerical Computation of the Large Deviation Multifractal Spectrum", in Proc. *CFIC*, Rome, Italy, 1996.
4. I.Reljin, B. Reljin, M. Avramov-Ivic, D. Jovanovic, G. Plavec, S. Petrovic and G. Bogdanovic, "Multifractal analysis of the UV/VIS spectra of malignant ascites: Confirmation of the diagnostic validity of a clinically evaluated spectral analysis", *Physica A: Statistical Mechanics and its Applications*, (387), pp 3563-3573, 2008.
5. M. Abadi and E.Grandchamp, "Large deviation spectrum estimation in two dimensions", *Multimedia Systems and Applications*, (31), 2007.
6. V. Delouille, P. Chainai s, J.F. Hochedez "Spatial and temporal noise in solar EUV observations", *Solar Physics*, (248), pp 441-455, 2008.
7. F. Mendoza, P. Verboven, Q. Tri Ho, G. Kerckhofs, M. Wevers and B. Nicola "Multifractal properties of pore-size distribution in apple tissue using X-ray imaging", *Journal of Food Engineering*, (99-2), pp 206-215, 2010.
8. J. Lévy Véhel, "Introduction to the Multifractal Analysis of Images", in Y. Fisher, editor, *Fractal Images Encoding and Analysis*, Springer-Verlag, 1998.
9. J. Lévy Véhel, B. Guiheneuf, "Multifractal Image Denoising", *SCIA*, 1997.
10. Y. Chen, Y. Dong, D. Lu and Y. Pan, "The Multi-fractal Nature of Worm and Normal Traffic at Individual Source Level", *Lecture notes in computer science*, (3495), pp 505-510, 2005.
11. J. Lévy Véhel, P. Legrand, "Signal and Image processing with FracLab", *Thinking in Patterns : fractals and related phenomena in nature*, World Scientific, 2004, pp. 321-322
12. B. Mandelbrot, "Intermittent Turbulence in Self-Similar Cascades: Divergence of High Moments and Dimension of the Carrier", *J. Fluid Mech.*, vol. 62, pp. 331-358, 1974.
13. B. Mandelbrot, *Fractals and Scaling in Finance*, Springer Verlag, 1997.
14. M. Ossiander, E. Waymire, "Statistical Estimation for Multiplicative Cascades", *Ann. Stat.*, vol. 28, no. 6, pp. 1533-1560, 2000.
15. J. Lévy Véhel, P. Mignot, "Multifractal Segmentation of Images", in *Fractals*, vol. 2, no. 3, pp. 371-378, June, 1994.